Synthesis and UV−Visible spectroscopy study of core−shell gold−palladium nanoparticles by iterative seeding of citrate

IOP Conf. Series: Materials Science and Engineering **496** (2019) 012020 doi:10.1088/1757-899X/496/1/012020

Synthesis and UV–Visible spectroscopy study of core–shell gold–palladium nanoparticles by iterative seeding of citrate

M B S Putra, E Saepudin and T A Ivandini

Department of Chemistry, Faculty of Mathematics and Natural Sciences (FMIPA), Universitas Indonesia, Depok 16424, Indonesia

Corresponding author: ivandini.tri@sci.ui.ac.id

Abstract. In this study, gold and palladium nanoparticles (Au NPs and Pd NPs) were successfully synthesized by the iterative seeding of citrate and ascorbate, respectively. UV–visible spectroscopy results revealed that Au NPs exhibit plasmonic resonance peaks at 540–560 nm, while Pd NPs exhibit peaks at 220 nm. Transmission electron microscopy images revealed particle size distributions of 19.3 ± 4.2 nm and 31.9 ± 6.1 nm for Au NPs and Pd NPs, respectively. Larger sizes were observed for palladium nanoparticles because of their aggregation caused by the deficiency of the capping agent, while gold particles exhibited size stability. Furthermore, gold–palladium (AuPd) nanoflower particles were synthesized by the iterative citrate seeding of Pd on the Au NP surface.

Keywords: Nanoparticle, Core–shell, Gold, Gold–palladium, Citrate seeding.

1. Introduction

Metal nanoparticles exhibit typically different properties from their corresponding bulk materials, which can be employed for many applications, including catalytic, optic as well as magnetic and sensing applications. These properties are affected by the shape of the nanoparticles. Therefore, control the shape and size is crucial factor in the synthesis of metal nanoparticles [1].

On the other hand, bimetallic heteronanostructures are known to provide synergic optic, electronic, and catalytic properties their monometallics. In some cases, a drastically improvement of properties was reported, such as at a gold and palladium bimetal [2].

Several studies have reported the synthesis of colloidal Au nanoparticles (Au NPs), including even some of the methods that start with the use of bulk metal. However, most of these methods begin with Au^{3+}, and using different reductants, particles of varying sizes are generated [3–5]. For example, reductants such as $NaBH_4$ or white phosphorus afford small Au particles with a diameter *d* of less than 10 nm [3]. Sodium citrate is the most widely used reductant. By the variation of the citrate: Au ratio, colloidal particles with d values ranging from 10 to 150 nm can be prepared [4]. On the other hand, the nucleation and growth of Pd nanoparticles (Pd NPs) have been successfully investigated using H_2PdCl_4 and *L*-ascorbic acid (AA) as the precursor and reductant, respectively [5]. This study focused on the synthesis of Au NPs, Pd NPs, and gold–palladium (AuPd) NPs (Au@Pd NPs). In addition, the comparison between their characteristics was discussed.

2. Experimental

2.1. Materials and instruments

Hydrogen tetrachloroaurate(III) ($HAuCl_4$), palladium chloride(II) ($PdCl_2$), and trisodium citrate ($Na_3C_6H_5O_7$) were purchased from Wako Pure Chemical Industries Ltd. Ultrapure deionized water with a resistivity of 18.2 MΩ·cm was obtained from a Millipore Direct® Q5-UV system.

UV–Visible spectra were recorded on a Thermo Scientific Multiskan GO system, and transmission electron microscopy (TEM) images were recorded on a Microscope Tecnai 200kV D2360 SuperTwin.

2.2. Preparation of Au-core/Pd-shell

2.2.1. Synthesis of Au NPs. Au NPs were synthesized using iterative citrate-seeded colloidal Au via the method reported by Brown and Natan with some modifications [3]. First, 100 mM of sodium citrate was added into a stirred solution of boiling 100 mL of 0.01% $HAuCl_4$. Second, this mixture was boiled until the solution reached the boiling point, followed by the dropwise addition of sodium citrate until the solution color changed from yellowish $HAuCl_4$ to dark red Au NPs. The solution was cooled with stirring for 10 min., and the solution color changed to red-pink, indicative of the complete reduction of $HAuCl_4$ into Au NPs.

2.2.2. Synthesis of Pd NPs. Pd NPs were synthesized using AA as the reductant. First, a solution of Pd(II) in 0.001 M of HCl was mixed with 0.1 M of fresh AA with vigorous stirring while simultaneously maintaining an extremely low temperature. Reaction completion was verified by the appearance of dark brown colloids of Pd NPs [6].

2.2.3. Synthesis of Au@Pd NPs. Au@Pd NPs were synthesized via the Hu *et al.* method reported previously [7]. Pd-coating procedures was performed by reduction reaction of Pd^{2+} solution by AA in the presence of Au NPs seeds. Briefly, an aliquot containing 30 mL of gold seeds was added into a flask containing 1.1 mL of 1.0 mM of H_2PdCl_4 and 9.9 mL of water. Second, the mixture was cooled down to ~4 °C in an ice bath with vigorous stirring. Then, 3.5 mL of 10 mM AA was slowly dropped in the mixture. After the addition of AA, the mixture was stirred for another 15 min. The mixture color gradually deepened from pinkish red for Au NPs to fully dark brown for coated Au@Pd NPs.

3. Results and discussion

3.1. Synthesis of Au, Pd, and Au@Pd NPs and its characterization

Au NPs were synthesized in one pot using 0.01% $HAuCl_4$ and 0.01 M sodium citrate as the precursor and reductant, respectively. Sodium citrate successfully reduced Au^{3+} into Au^0 nanoparticles at the boiling point of the solvent, leading to a color change from yellowish $HAuCl_4$ into pinkish-red Au^0. The reaction kinetics can be expressed by the following equation [8]:

$$Au^{3+} + Na_3C_6H_5O_7 \rightarrow Au^0 + 3Na^+ + citr \quad (1)$$

The UV–vis spectrum of colloidal Au NPs exhibiting a plasmon resonance peak at ~522 nm together with the TEM image of Au NP are shown in figure 1a and figure 1b, respectively. The correlation of the data revealed that the surface plasmon resonance of Au NPs is relative to the particle size as shown by the TEM image, which was ~19 nm with a standard deviation of 4.3 nm [9]. Kwolek and Wojnicki [10] have reported the size of this Au NPs is suitable as the core of a composite. Peak shifting was not observed (figure 1c), indicating that the Au NP size is stable with the increasing content of gold ions, i.e., double and triple the Au NP concentrations, which was probably related to the presence of citrate as the capping and reducing agent.

Meanwhile, Pd NPs (figure 2) has completely different spectrum compare with Au NPs. In the UV–vis spectrum shown in figure 2a for the obtained colloidal Pd NPs, two peaks were observed at ~220 nm and 246 nm, respectively, for the least amount of the reductant. The first peak corresponded to Pd(II) ions, whereas the second peak corresponded to AA. Both peaks were absent, indicative of the complete reduction of Pd, while the peak intensity increased at 300–400 nm, corresponding to Pd NPs (brownish dark). As shown in figure 2a, this Pd NPs peak is not observed, which was related to the low concentrations of the formed Pd NPs. TEM images (figure 2b, figure 2c and figure 2d) revealed a mean particle size of 31.9 nm with a standard deviation of ±6.1; this value is greater than that of the

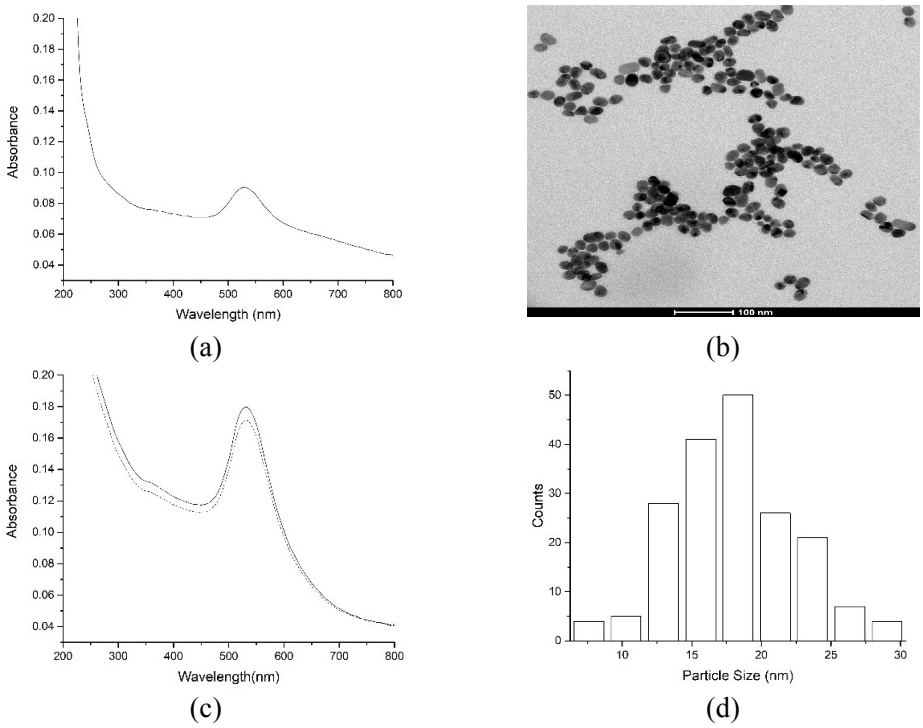

Figure 1. (a) UV–visible spectrum of Au NPs, (b) TEM image of Au NPs with 250× magnification, (c) UV–visible spectrum of Au NP at double (dash - - -) and triple concentrations (line —), and (d) particle size distribution of Au NPs.

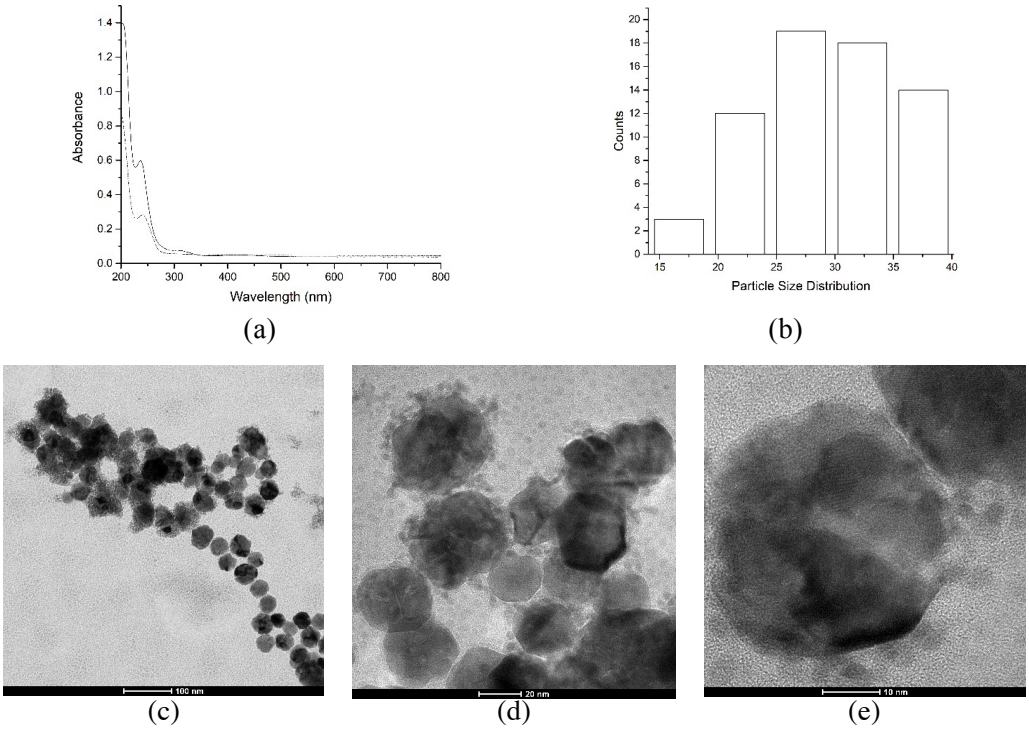

Figure 2. (a) UV–visible spectrum of H_2PdCl_4 (Line —) and Pd NPs (Dash - -), in addition to that of *L*-ascorbic acid, (b) particle size distribution of Pd NPs, (c) TEM images, and (d and e) HRTEM images of Pd NPs.

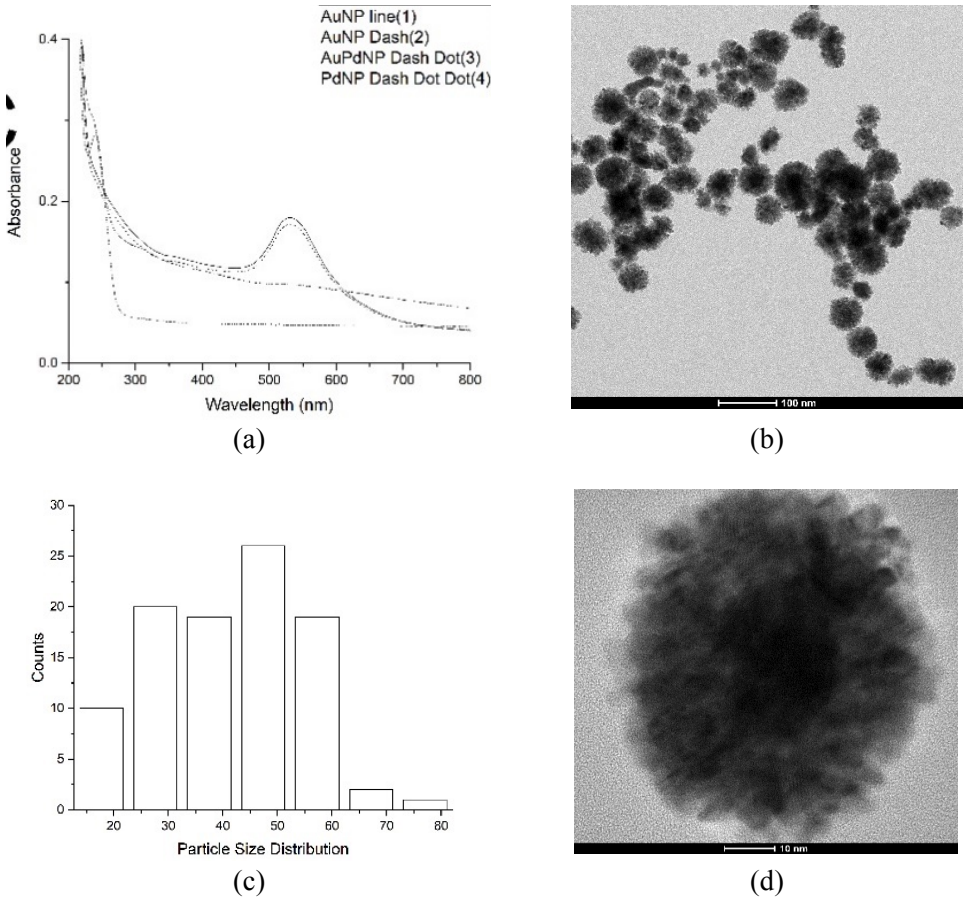

Figure 3. (a) Comparison of the UV–visible spectra of Au NPs, Pd NPs, and Au@Pd NPs, (b) TEM image of Au@Pd NPs and (c) its size distribution, and (d) HRTEM image of Au@Pd NPs.

Au NPs. The deficiency of the capping agent of Pd NPs tended to produce nanoparticle aggregates [5,6]. Despite their size, Pd NPs still exhibited catalytic property [2]. The reduction of Pd(II) as confirmed by the change in color confirmed the nucleation and growth of particles. Wojnicki *et al.* [5] have proposed two steps related to the reduction of Pd(II) to Pd(0) (nucleation) and auto-growth of Pd NPs:

$$Pd(II) + AA \rightarrow Pd(0) + DHA \quad (2)$$

$$Pd\ (II) + AA + Pd(0) \rightarrow 2Pd(0) + DHA \quad (3)$$

The comparison of the UV–visible spectra of the Au NPs, Pd NPs, and Au-core/Pd-shell NPs is shown in figure 3a. Wang [2] has reported that the optical properties of the Au@Pd core–shell nanostructures are strongly dependent on the thickness and morphology of the Pd shells. The figure clearly revealed the disappearance of the Au NP plasmon resonance peak at 522 nm for the Pd-shell-covered Au NPs. To examine the nanoparticle size, TEM and HRTEM images were recorded. The TEM images have shown in figure 3b and figure 3c revealed spherical particles with an average particle size of 45 ± 13.7 nm. The Pd-shell layer thickness determined by HRTEM images was calculated to be ~15 nm with a gold core diameter of ~23 nm [11,12], indicating that some Au NP aggregates are formed in case of Pd-shell-covered Au NPs. The HRTEM image also revealed the successful synthesis of the Au-core/Pd-shell nanoflower structure.

4. Conclusions

Au NPs, Pd NPs, and Au@Pd NPs were successfully synthesized by the iterative seeding of citrate and reduction using *L*-AA, leading to Au NPs, Pd NPs, and Au@Pd NPs with sizes of 19 ± 4.2 nm, 31 ± 6.1 nm, and 45 ± 13.7 nm, respectively. The Pd-shell covering the Au NPs successfully afforded a nanoflower structure for the Au@Pd NPs.

Acknowledgements

This research was funded by PITTA Grant 2017 from Universitas Indonesia with contract number 1822/UN.R3.1/PPM.00.01/2017. The authors would like to thank Einago (www.einago.com) for the English language review.

References

[1] Nikkoobakht B and El-Sayed M A 2003 *Chem. Mater.* **15** 1957–62
[2] Jing H and Wang H 2014 *Cryst. Eng. Comm.* **16** 9469–77
[3] Brown K R, Walter D G and Natan M J 2000 *Chem. Mater.* **12** 306–13
[4] Luty-Błocho M, Pacławski K, Wojnicki M and Fitzner K 2013 *Inorg. Chim. Acta* **395** 189–96
[5] Wojnicki M, Fitzner K and Luty-Błocho M 2016 *J. Colloid Interface Sci.* **465** 190–9
[6] Wojnicki M, Pacławski K, Rudnik E and Fitzner K 2011 *Hydrometallurgy* **110** 56–61
[7] Hu J W, Li J F, Ren B, Wu D Y, Sun SG and Tian Z Q 2007 *J. Phys. Chem. C* **111** 1105–12
[8] Pacławski K, Streszewski B, Jaworski W, Luty-Błocho M and Fitzner K 2012 *Colloids Surf. A Physicochem. Eng. Asp.* **413** 208–15
[9] Moraes Silva S, Tavallaie R, Sandiford L, Tilley R D and Gooding J J 2016 *Chem. Commun.* **52** 7528–40
[10] Kwolek P and Wojnicki M 2014 *J. Photochem. Photobiol. A Chem.* **286** 47–54
[11] Ma T, Liang F, Chen R, Liu S and Zhang H 2017 *Nanomaterials* **7** 239
[12] Harpeness R and Gedanken A 2004 *Langmuir* **20** 3431–4